

# The Photocatalytic Applications of $\text{TiO}_2\text{-WO}_3$ Heterostructure in Methylene Blue

Guangyuan Hai<sup>a</sup>, Haiming Zhang<sup>b\*</sup>

<sup>a,b</sup>Tiangong University, School of Physical Science and Technology, TianJin, 300387, CHN

<sup>a</sup>Email: [haiguangyuan@foxmail.com](mailto:haiguangyuan@foxmail.com)

<sup>b</sup>Email: [zhmtjwl@163.com](mailto:zhmtjwl@163.com)

## Abstract

In this work,  $\text{TiO}_2\text{-WO}_3$  composite materials were forged by sol-gel method and the forged samples were characterized by X-ray diffraction, X-ray photoelectron spectroscopy, scanning electron microscopy and UV-vis diffuse reflectance spectroscopy. The tough interaction in the interface of  $\text{TiO}_2\text{-WO}_3$  heterostructures and the solar spectral response of  $\text{TiO}_2$  and  $\text{WO}_3$  reduce the electron-hole pair recombination rate and enhance the photoelectrochemical activity. The  $\text{TiO}_2\text{-WO}_3$  heterostructures also show good adsorption ability for organic pollutants. This study testified that the fabricated  $\text{TiO}_2\text{-WO}_3$  heterostructures are expectation materials for efficient water splitting as well as adsorption and photocatalytic wipe off organic pollutants.

**Keywords:** titania dioxide; tungsten trioxide; photocatalytic; methylene blue.

## 1. Introduction

In recent years, photocatalysis technology has received widespread attention on account of its applications in organic synthesis and the abatement of pollutants in water and air [1]. It is applied to wipe off the organic pollutant which includes detergent, dyes, pesticides and herbicides under UV-light irradiation. The heterogeneous photocatalyst attracted a crucial attention due to elimination of organic pollutants in water [2-5] and semiconductor photocatalysts drew attention because of inexpensive and environmental friendliness.

---

\* Corresponding author

Photocatalysis is used to eliminate pollutants by conversion of optical energy into the electrochemical energy required for photo-oxidation by a catalyst[6]. Titanium dioxide ( $\text{TiO}_2$ ) is demonstrably the most promising material for applications to air and water purification from various pollutants [7]. However,  $\text{TiO}_2$  only works in conjunction with irradiation of limited wavelength:  $\text{TiO}_2$  band gap ( $E_g \approx 3.2$  eV) requires  $\lambda < 385$  nm, which rules out 95% of the solar spectrum. Moreover, the rapid recombination of the photocatalytically produced charge carriers competes with the electron transfer of the reactants adsorbed on the catalyst surface, which makes it not fit for efficient utilization[8]. A large number of methods have been used to increase the photocatalytic property of  $\text{TiO}_2$  for instance doping with metal or metal oxides, noble metal deposition and anion doping etc. Among semiconductor oxides, crystalline tungsten oxide ( $\text{WO}_3$ ) has some advantages including: induction of surface acidity to promote adsorption of  $\text{OH}^-$ ; water and pollutant molecules; its band gap is short (2.6-2.8 eV), thus requiring longer wavelengths for the excitation [9]. The lower conduction band (CB) position of  $\text{WO}_3$  than that of  $\text{TiO}_2$  accelerates the electron transfer from  $\text{TiO}_2$  to  $\text{WO}_3$  and the holes transfer in opposite direction. The idea of coupling  $\text{TiO}_2$  with another metal oxide with appropriate band gap and edge positions can be used as a feasible channel to promote photoproduced charge separation. Pandi and Gopinathan[10] fabricated  $\text{TiO}_2/\text{WO}_3$  synthetic material by hydrothermal synthesis and surface modification. The enhanced decomposition of aqueous eosin-Y with  $\text{TiO}_2/\text{WO}_3$  was because of visible light absorption and decreased carrier recombination rate. Ke et al.[11] fabricated  $\text{TiO}_2/\text{WO}_3$  synthetic material hydrothermally with CTAB as a surfactant. The  $\text{TiO}_2/\text{WO}_3$  disintegrated 100% of RhB in 50 min. Riboni and his colleagues [12] prepared  $\text{WO}_3\text{-TiO}_2$  mixed oxide by a sol-gel method. The photocatalyst with the optimum tungsten content of 3% had higher activity than  $\text{TiO}_2$  P25 and degraded 31% acetaldehyde in 2 h in the gas phase under mainly visible irradiation. Similarly, Eibl and his colleagues [13] state that  $\text{WO}_3$  is formed in tungstated titania when the tungsten loading exceeds a mass fraction of 20% and the powders are calcined above 923 K. In summary, the literature has inadequately characterized the  $\text{TiO}_2/\text{WO}_3$  semiconductor catalyst. In this work, we fabricated  $\text{WO}_3$  by hydrothermal method and fabricated  $\text{TiO}_2$ 、 $\text{TiO}_2\text{-WO}_3$ . The fabricated samples were characterized by various techniques for example X-ray diffraction(XRD), X-ray photoelectron spectroscopy (XPS), scanning electron microscope (FESEM) and UV-vis diffuse reflectance (UV-Vis-DRS) spectroscopy. The prepared  $\text{TiO}_2\text{-WO}_3$  heterostructures have predominant interfacial interactions with tunable electrical property and show better photocatalytic activity. The  $\text{TiO}_2\text{-WO}_3$  hetero structures also show good degradation competence towards the organic pollutant, methylene blue (MB).

## **2. Materials and Methods**

### **2.1. Chemicals**

Ammonium tungsten partial, Ammonium metatungstate hydrate (AMT); Tetrabutyl titanate(TBOT); ethyl alcohol absolute( $\text{C}_2\text{H}_6\text{O}$ ); hydrochloric acid(HCl); Acetic Acid( $\text{CH}_3\text{COOH}$ ) ; methylene blue(MB); All chemicals and reagents were of analytical grade and were used as such without further purification, and double distilled water was used throughout this work.

### **2.2. Catalyst preparation**

Tungsten trioxide ( $\text{WO}_3$ ) powder was prepared by hydrothermal method. Weigh ammonium metatungstate

(AMT) and add it to 20mL of deionized water, stirring constantly until dissolved. Then add hydrochloric acid to the resulting solution to adjust the pH to 2. After stirring the solution for half an hour, transfer the solution to a 100 mL high-pressure reactor, put the high-pressure reactor into a drying oven, and keep the oven at 180°C for 24 hours. After cooling the reactor to room temperature, take out the product and centrifuge and wash the product. First wash with deionized water for three times and then wash with anhydrous ethanol for three times. Then dry at 80°C, grind the dried products to obtain pale yellow powder products. TiO<sub>2</sub> powder was prepared by sol-gel method. Tetrabutyl titanate was added into anhydrous ethanol and stirred for 20 min to obtain yellow clarification solution A. Deionized water and glacial acetic acid were added into anhydrous ethanol, and proper amount of nitric acid was added after full stirring. PH value was adjusted to 2 to obtain solution B. Then under the intense mixing, mixing solution A and solution B, fully mixing stand for 24 hours, after get the gel after place into the oven, drying under 80°C temperature, then put the samples in under 550 °C heat treatment resistance furnace, heating speed 2°C per minute, after the heat treatment of samples of grinding end up with white powder.

### 2.3. Photocatalytic activity

Photocatalytic activity test was performed as follows. 0.3g WO<sub>3</sub>/TiO<sub>2</sub>/WO<sub>3</sub>-TiO<sub>2</sub> composites were added to 300 mL MB (300 mg/L) aqueous solution and the suspension solution was stirred in the dark for 30 min until the adsorption/desorption process reached equilibrium. Xe lamp was employed as the UV-visible light source, and it was placed 14 cm away from the solution. In every 20 min, 5 mL of the solution was taken away and the suspension was removed by using centrifugation. Then measuring the maximum absorbance at 665 nm of the MB by the spectrophotometry. The degradation rate was calculated using  $E = (1 - C/C_0)$ , where C<sub>0</sub> and C are the MB concentrations before and after photodegradation with UV-visible light.

### 3. Results and discussion

Control TiO<sub>2</sub> phase (**Figure.1a**) is pure anatase with a tetragonal structure (JCPDS # 01-083-0950). Control WO<sub>3</sub> (**Figure.1b**) exhibits main peaks indexed as monoclinic crystalline structure (JCPDS # 01-083-0950). In the TiO<sub>2</sub> sample the diffraction peak of [101] at  $2\theta = 25.28^\circ$  and the peak of [200] of WO<sub>3</sub> at  $2\theta = 24.36^\circ$  are the highest intense, show that [101,200] are the most growth orientations. As evident from the XRD patterns (**Figure.1c**) the main anatase peaks [101,103,200,105,213] at  $2\theta = 25.3^\circ, 37.9^\circ, 48.4^\circ, 53.9^\circ, 62.7^\circ$  and the monoclinic form peaks [200,220,222,400,420,422] at  $2\theta = 23.6^\circ, 33.6^\circ, 41.5^\circ, 48.4^\circ, 54.6^\circ, 60.3^\circ$ . Besides, no phase transformation of TiO<sub>2</sub> or of WO<sub>3</sub> occurred during the compound of the hybrid powders: in all the samples TiO<sub>2</sub> maintained the anatase structure, while WO<sub>3</sub> kept the monoclinic form.

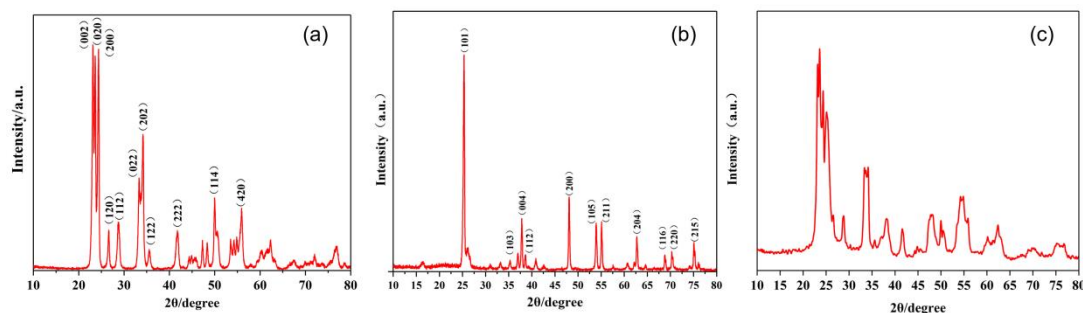


**Figure 1:** (a) XRD patterns of  $\text{WO}_3$  (b) XRD patterns of  $\text{TiO}_2$ , (c) XRD patterns of  $\text{TiO}_2$ - $\text{WO}_3$  heterostructures.

We report the field emission scanning electron microscope (SEM) micrographs of control  $\text{TiO}_2$  and  $\text{WO}_3$  and hybrid  $\text{TiO}_2$ - $\text{WO}_3$  powders calcined at  $550^\circ\text{C}$  **Figure. 2**.

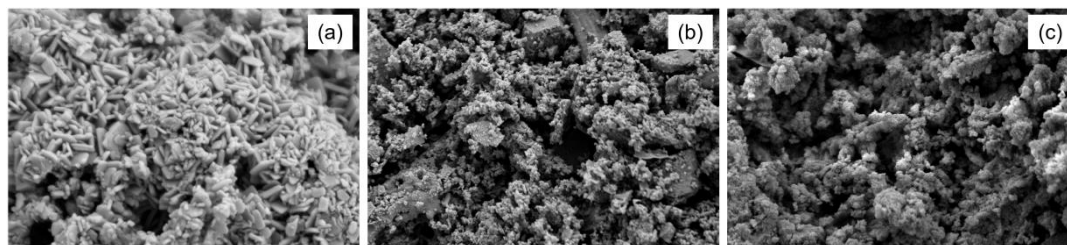


**Figure 2:** (a) SEM images of  $\text{WO}_3$  (b) SEM images of  $\text{TiO}_2$  (c) SEM images of  $\text{TiO}_2$ - $\text{WO}_3$  heterostructures.

X-ray photoelectron spectroscopy (XPS) was applied to further research the chemical and bonding environment of the composite powders. **Figure.3 a** presents a low-resolution full range XPS spectrum of the  $\text{TiO}_2$ - $\text{WO}_3$  composite powders. The XPS survey spectrum showed that the distinctive as well as the Auger peaks of Ti, O, W and the combined material confirmed the presence of titanium, oxygen, tungsten. The  $\text{Ti}2p$  high resolution XPS spectra are analyzed in **Figure.3 b**. The binding energies of 459.6 and 465.25 eV are state that  $\text{Ti}2p_{3/2}$  and  $\text{Ti}2p_{1/2}$  separately. The splitting of the 2p doublet was 5.65 eV, reveal a normal state of  $\text{Ti}^{4+}$  in the  $\text{TiO}_2$ - $\text{WO}_3$  composite powders. The high-resolution  $\text{W}4f$  XPS (**Figure.3 c**) shows the peaks at 38.4 and 36.3 eV corresponding to the characteristic  $\text{W}4f_{5/2}$  and  $\text{W}4f_{7/2}$  components respectively in  $\text{WO}_3$ . The energy gap between these two peaks is 2.1 eV which suggested the  $\text{W}^{6+}$  oxidation state in  $\text{WO}_3$ . The XPS results confirm the superior interaction between  $\text{TiO}_2$  and  $\text{WO}_3$  through the formation of Ti-O-W bonds in  $\text{TiO}_2$ - $\text{WO}_3$  heterostructures. With respect to the XPS spectra of O1s in **Figure.3 d**, the O1s peak at 530.95 eV is attributed to  $\text{O}^{2-}$ .

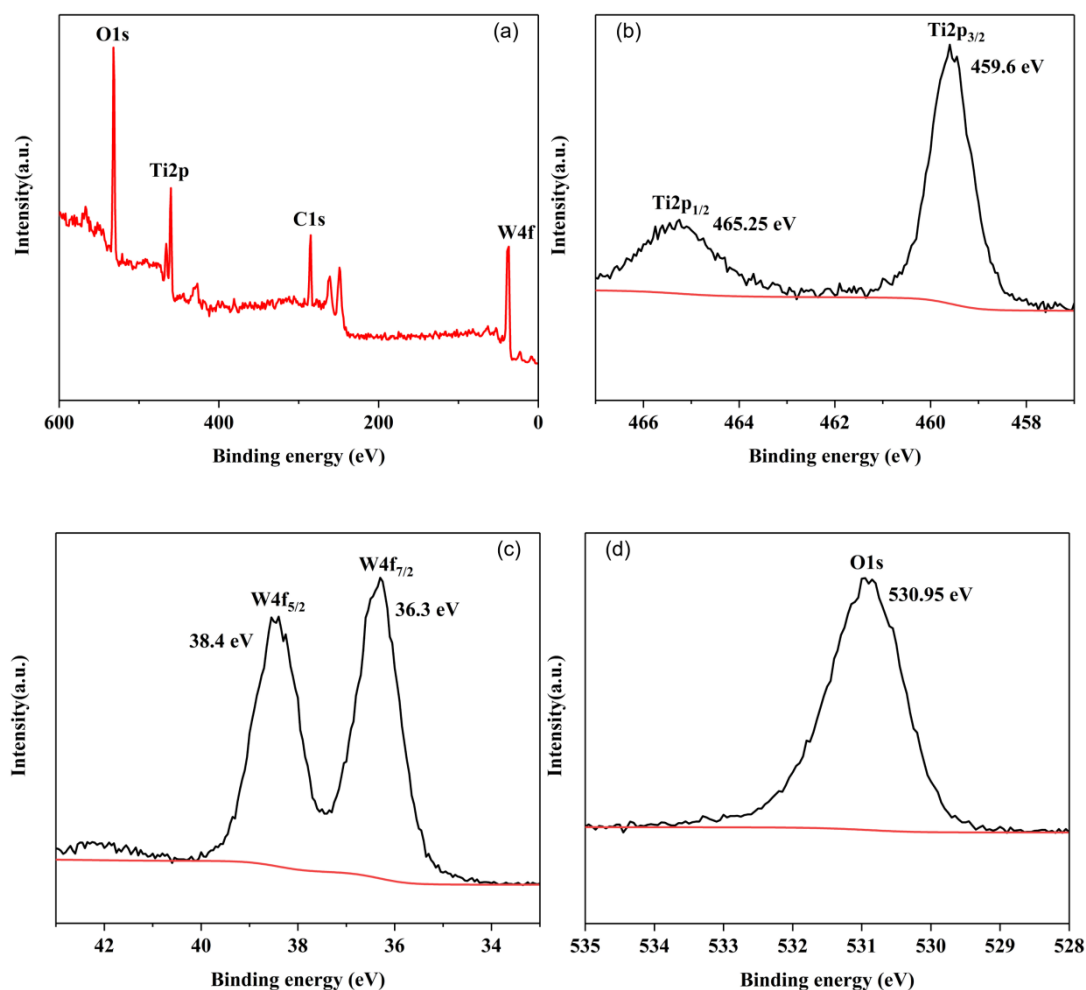


**Figure 3:** XPS spectra of the  $\text{TiO}_2\text{-WO}_3$  heterostructures: (a) fully scanned spectra; (b) XPS spectra of Ti2p; (c) XPS spectra of W4f (d) XPS spectra of O1s.

The UV-Vis-DRS spectrum was recorded to understand the light absorption property of the samples and shown in **Figure.4 a**. The re-reflectance of  $\text{TiO}_2\text{-WO}_3$  heterostructures reduced with the addition of  $\text{WO}_3$  content which revealed the enhanced absorption of the incident light. We used Tauc diagram to calculate the band gap of the prepared samples. The transformed Kubelka-Munk function,  $[F(R)h\nu]^{1/2}$  ( $F(R) = (1-R)^2/2R$  and  $R$  is the reflectance) was plotted against the energy of light,  $h\nu$ . The intercepts of the tangent drawn at absorption function to the energy axis at zero absorption are evaluated to get the band gap values[15]. The band gap of  $\text{TiO}_2$  and  $\text{WO}_3$  was 3.12 eV(**Figure.4 c**) and 2.52 eV(**Figure.4 b**), and the  $\text{TiO}_2\text{-WO}_3$  heterostructures band gap was 2.36 eV(**Figure.4 d**). The fractionally reduced band gap values in  $\text{TiO}_2\text{-WO}_3$  heterostructures compared to pure  $\text{TiO}_2$  shows the hard interaction between  $\text{TiO}_2$  and  $\text{WO}_3$ . The strong mutual effect can availably hinder the recombination of  $e^-h^+$  through the  $\text{TiO}_2\text{-WO}_3$  heterojunction.

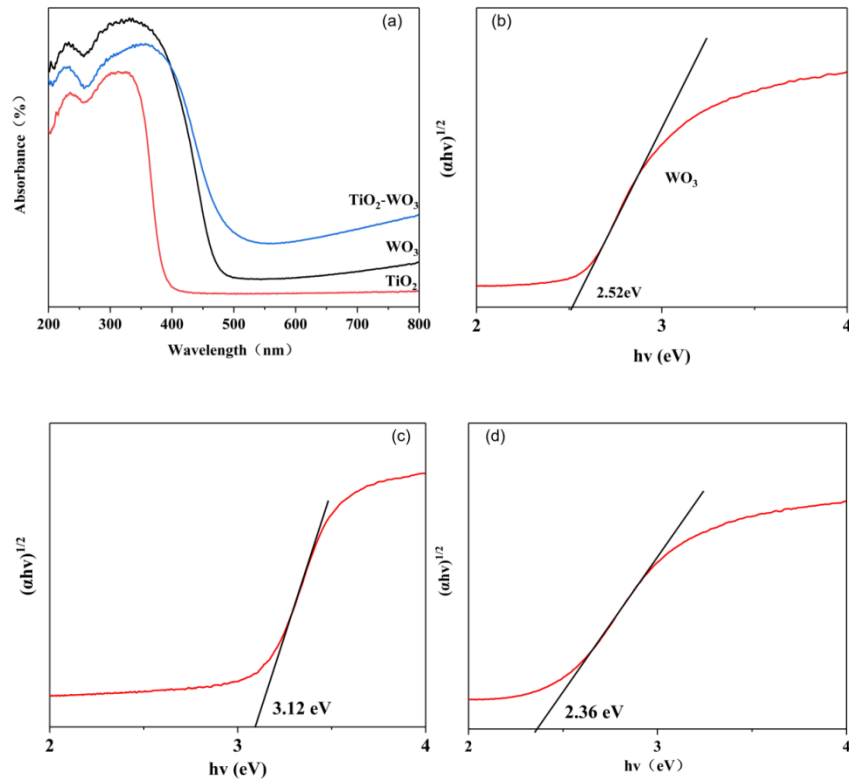


**Figure 4:** (a) UV-Vis-DRS spectra of TiO<sub>2</sub>, WO<sub>3</sub> and TiO<sub>2</sub>-WO<sub>3</sub> (b) (c) (d) Tauc plot of TiO<sub>2</sub>, WO<sub>3</sub> and TiO<sub>2</sub>-WO<sub>3</sub> heterostructure.

**Figure.5** shows photocatalytic activity of as-prepared TiO<sub>2</sub>, WO<sub>3</sub> and TiO<sub>2</sub>-WO<sub>3</sub>. It can be observed that TiO<sub>2</sub>-WO<sub>3</sub> possesses the highest photocatalytic degradation rate (99% within 100 min), which is higher than that of WO<sub>3</sub> (57%) and TiO<sub>2</sub> (25%) at the same condition.

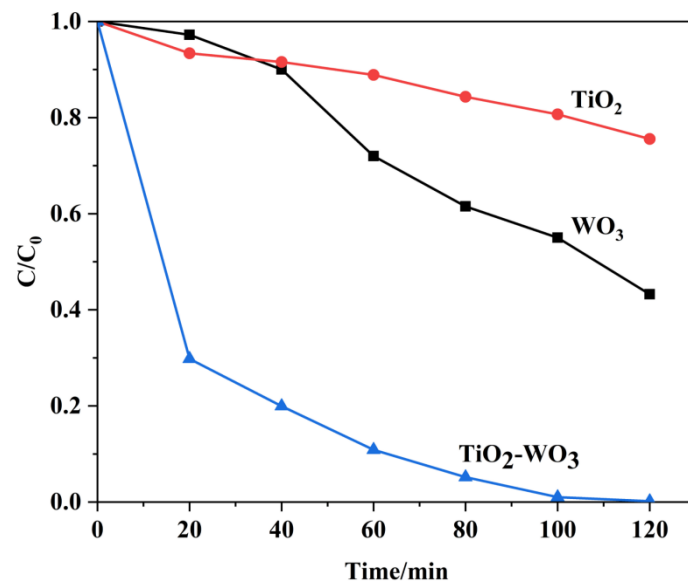


**Figure 5:** Photodegradation of Methylene blue in the presence of TiO<sub>2</sub>, WO<sub>3</sub> and TiO<sub>2</sub>-WO<sub>3</sub> composites.

#### 4. Conclusions

A simple sol-gel method followed by calcination process was used to synthesize  $\text{TiO}_2\text{-WO}_3$  heterostructures with superior interfacial interactions. The  $\text{TiO}_2\text{-WO}_3$  showed almost complete removal of MB in 100 min under visible light by photocatalytic and adsorption processes suggesting the higher adsorption of MB on the surface of  $\text{TiO}_2\text{-WO}_3$  heterostructures. The band gap of  $\text{TiO}_2$  reduced from 3.12 eV to 2.36 eV in the  $\text{TiO}_2\text{-WO}_3$  heterostructures which show the formation of heterojunction, and resulted in the reduction of recombination of  $e^-h^+$  pair.  $\text{TiO}_2$  and  $\text{WO}_3$  act in synergy: due to the difference in band possible of the semiconductors, electrons shift from the conduction band of  $\text{TiO}_2$  to that of  $\text{WO}_3$  upon UV light irradiation. This research projects  $\text{TiO}_2\text{-WO}_3$  heterostructures with great promise solar and visible light active materials for efficient water splitting as well as adsorption and photocatalytic reduce of organic pollutants.

#### Acknowledgement

Thanks to Professor Haiming Zhang and my classmate Yuxuan Sun for they guidance during the research process.

#### References

- [1]. R. Abazari, A.R. Mahjoub, L.A. Saghatforoush, S. Sanati, *Mater. Lett.* 133, 208-211 (2014)
- [2]. S. Malato, P. Fernandez-Ibanez, M.I. Maldonado, J. Blanco, W. Gernjak, Recent overview and trends. *Catal. Today* 147, 1-59 (2009)
- [3]. M.A. Rauf, S.S. Ashraf, Fundamental principles and application of heterogeneous photocatalytic degradation of dyes in solution. *J. Chem. Eng.* 151, 10-18 (2009)
- [4]. A.R. Khataee, M.B. Kasiri, Photocatalytic degradation of organic dyes in the presence of nanostructured titanium dioxide: influence of the chemical structure of dyes. *J. Mol. Catal. A Chem.* 328, 8-26 (2010)
- [5]. S. Ahmed, M.G. Rasul, W.N. Martens, R. Brown, M.A. Hashib, Advances in heterogeneous photocatalytic degradation of phenols and dyes in wastewater: a review. *Water Air Soil Pollut.* 215, 3-29 (2011)
- [6]. L. Gao, W. Gan, Z. Qiu, X. Zhan, T. Qiang, J. Li, Preparation of heterostructured  $\text{WO}_3/\text{TiO}_2$  catalysts from wood fibers and its versatile photodegradation abilities, *Sci. Rep.* 7 (2017) 1102.
- [7]. D. Spanu, S. Recchia, S. Mohajernia, P. Schmuki, M. Altomare, Site-selective Pt dewetting on  $\text{WO}_3$ -coated  $\text{TiO}_2$  nanotube arrays: an electron transfer cascade-based  $\text{H}_2$  evolution photocatalyst, *Appl. Catal. B: Environ.* 237 (2018) 198-205.
- [8]. J. M.V. Dozzi, S. Marzorati, M. Longhi, M. Coduri, L. Artiglia, E. Selli, Photocatalytic activity of  $\text{TiO}_2\text{-WO}_3$  mixed oxides in relation to electron transfer efficiency, *Appl. Catal. B: Environ.* 186 (2016) 157-165.
- [9]. N.A. Ramos-Delgado, L. Hinojosa-Reyes, I.L. Guzman-Mar, M.A. Gracia-Pinilla, A. Hernandez-Ramirez, Synthesis by sol-gel of  $\text{WO}_3/\text{TiO}_2$  for solar photocatalytic degradation of malathion pesticide, *Catal. Today* 209 (2013) 35-40.

- [10]. P. Pandi, C. Gopinathan, Synthesis and characterization of  $\text{TiO}_2$ -NiO and  $\text{TiO}_2$ - $\text{WO}_3$  nanocomposites, J. Mater. Sci.: Mater. Electron. 28 (2017) 5222-5234.
- [11]. D. Ke, H. Liu, T. Peng, X. Liu, K. Dai, Mater. Lett. 62 (2008) 447-450.
- [12]. F. Riboni, L.G. Bettini, D.W. Bahnemann, E. Selli,  $\text{WO}_3$ - $\text{TiO}_2$  vs.  $\text{TiO}_2$  photocatalysts: effect of the W precursor and amount on the photocatalytic activity of mixed oxides, Catal. Today 209 (2013) 28-34.  
L. Baia, E. Orban, S. Fodor, B. Hampel, E.Z. Ked.
- [13]. S. Eibl, B.C. Gates, H. Knozinger, Langmuir 17 (2001) 107-115.